EXPERIMENTAL INVESTIGATIONS ON THE ADAPTATION ACCURACY OF ADAPTIVE SLOTS IN WIND TUNNEL TEST SECTION WALLS

Meyer O, Blume S, Nitsche W
Institute of Aero- and Astronautics (ILR), Technical University (TU) Berlin, Germany

Keywords: *wind tunnel, adaptive test section, adaptive slots, adaptive walls*

Abstract

In many wind tunnel experiments the flow is affected by the presence of test section walls. These wall interferences can be minimized by correcting the measured model pressures or by influencing the model flow directly by means of ventilated or adaptive test section walls. The most successful technique of flexible, adaptive walls is still restricted to small research wind tunnels due to its mechanical complexity. However, a very promising alternative is the use of adaptive slots in test section walls.

This paper presents the latest experimental results on the effectiveness of adaptive slots. The experiments were conducted under high subsonic flow conditions in the new slotted test section of the transonic wind tunnel at TU Berlin's Aeronautical Institute (ILR).

The results presented focus on detailed investigations of the slot flow itself and the 2D slot adaptation of a 2D model (CAST7 airfoil). The in-slot investigations show the cause for the reduced adaptation effectiveness of slotted test sections, depending on the slot and flow parameters. The derived adaptation corrections minimise the observed deviations. The fully adapted flows around the airfoil coincide in both test sections (2D-adaptive and slotted) with an experimental error of about 2%.

1 Introduction

In many wind tunnel experiments, interactions (i.e., interferences) occur between the test section walls and the model flow. The flow field, and hence the measurements (pressures/ velocities), no longer experiences natural free flow conditions. Thus, all measured results must be corrected arithmetically afterwards or the flow itself must be corrected (i.e., adapted) during the test by means of mechanical measures, i.e., ventilated or flexible walls [2]. The objective of the latter techniques is to achieve free flow conditions around the tested model by 'streamlining' the flow to approximately free flow conditions in the vicinity of the walls and hence in the whole test section area. This is achieved either by passive (ventilated) or active-adaptive (flexible) test section walls. The method of adaptive/flexible walls yields the best adaptation results but is used in only a few research test sections due to its costly application in large-scale wind tunnels [12].

One promising alternative is to install test sections with adaptive longitudinal slots [10]. With this method, only small slots in the solid wall are deflected. This technique can be understood as a combination of the conventional passive slotted wall and the flexible wall method. It grants the opportunity to apply a superior adaptation strategy even to large scale test sections. The concept is to use flexible adaptive slot inserts to guide the model flow into free flow conditions and – using all four test section walls – even fully 3D adaptations become feasible [9] with a comparably lower complexity as other alternatives show [5]. Consequently, further advantages are that even existing passive slotted test sections could be converted to adaptive slotted test sections.

In principle, the slot adaptation works as follows: In a first step the wall pressures are measured in the test section with straight walls. These pressures are used in the second step to determine the required wall deflections from the

calculated wall interference with common single-step potential adaptation procedures for adaptive walls. Amecke's [1] method for 2D-flows and Holst's procedure [6] for 3D-flows are utilized. Afterwards, the wall deflections are transferred to slot deflections by a simple area rule which considers each individual slot configuration. The additional or reduced area for an adaptation in each cross section of the test section, formerly achieved by a deflected wall, must now be attained by the appropriate slot deflections. The area rule is illustrated in Fig.-1.

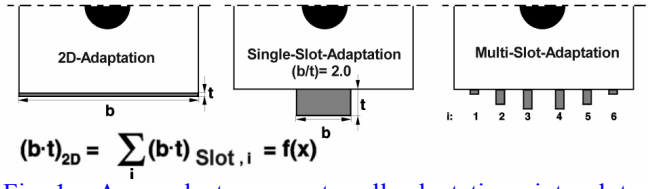

Fig.-1: Area rule to convert wall adaptations into slot adaptations

The flow in the slotted test section is now characterized by particular slot-typical parameters. In this case, the quality of an adaptation depends on the number, the cross-sectional distribution, and the relative width of the slots.

2 Adaptation quality of adaptive slots – a brief outline of the status quo

Previous numerical studies [3], [8], [10] and basic experiments [8], [9] demonstrated that adaptive slots work well. However, these studies also indicate a growing number of problems in case of particular test parameters (such as relative slot width and Mach number). Fig.- 2 illustrates the calculated pressure distributions for a Cast7 airfoil and the corresponding flow fields in the cross sectional area of the test section for M_∞=0.6. The pressure values of the slot adapted cases show only minor deviations compared to the 2D adaptation of maximum 3%. The flow fields below show increasing deviations inside and in the vicinity of the slots, especially decreasing assimilation of mass flow in the slender slots.

The more special experiment was focused on a comparison of bump flow fields using particular wall/slot deflections to find a correlation between slot geometries, Mach number and adaptation accuracy. The wall deflections were transferred via the area rule to the slot. Depending on the test parameters, certain velocity deviations in the slotted test section could be observed [9]. The analysis of the flow deviations around the bump shows a clear dependency on the test parameters slot width and Mach number, Fig.- 3. These deviations increase with decreasing slot width and decreasing Mach number.

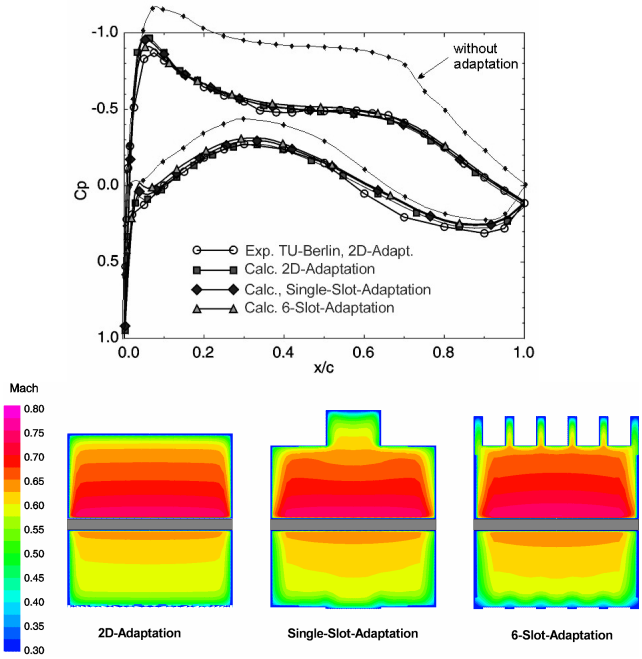

Fig.- 2: Calculated pressure distributions and flow fields for different adaptation strategies, Cast7 airfoil, M_∞=0.6, α=1°

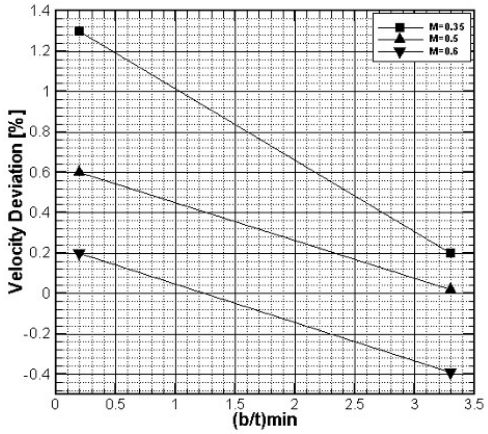

Fig.- 3: Velocity deviation in single-slotted/2D test section over a bump

The average velocity observed over the bump increases with decreasing slot width and decreasing Mach number. These phenomena match in absolute value with the numerical observations (see Fig.- 2 and [3]).

The reason for these negative effects and a methodology to possibly overcome or at least to correct the deviation in adaptation will be investigated in the present paper. Various detailed measurements of the slot flow are aimed on a better understanding of the accommodated mass flow in the slot, how it depends on the parameters used, and in what magnitude it influences the adaptation accuracy in the test section. A derived correction function will describe the influence of the used parameters. The following adaptations with well known test bodies will show the adaptation ability of adaptive slotted test sections using the previously developed correction. The following sections will present the latest experimental results and a discussion of the tests.

3. Slotted test section

The new slotted test section has single longitudinal slots in the floor and ceiling equipped with flexible inserts. The width of the slot and the test section are 40mm and 150mm, respectively. The maximum achievable slot depth is 48mm and therefore the relative slot width is $(b/t)_{min}$=0.83. The relative slot width can further be reduced by using rigid slot inserts. The slot is moved by DC-motors with gear drives. The position is measured by potentiometric displacement transducers. Fig.- 4 shows the test section from the side with access windows for optical measurements. The picture also shows the Cast7 airfoil fitted in the test section. The general layout is based on the existing 2D-adaptive test section of the ILR [4].

The slot is adjusted by 13 motors and displacement transducers. The adaptation calculation is performed over 45 pressure taps in the non-displaced slot. The side walls of the upper slot are made of glass to allow for detailed Laser-2-Focus anemometry inside the slot. To facilitate measurements around the tested bodies, the test section side walls are also made of glass. Fig.- 5 shows the cross-sectional area of the test section and the mechanical arrangement of the slot adjustment.

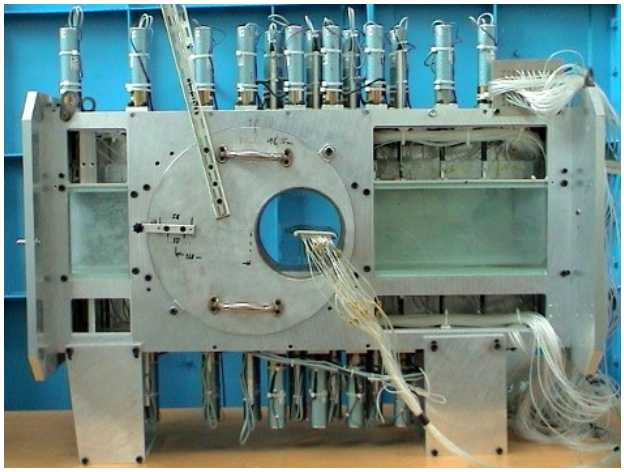

Fig.- 4: Side view of the test section

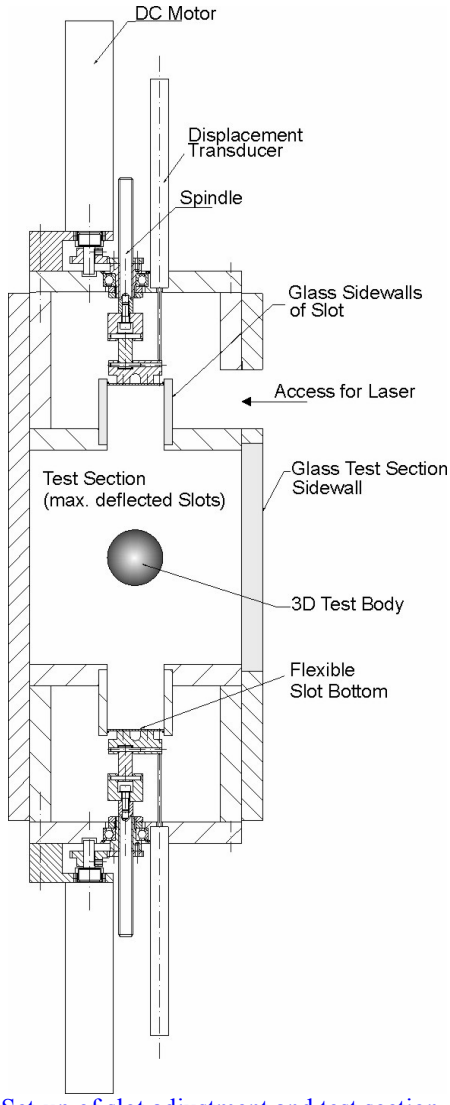

Fig.- 5: Set-up of slot adjustment and test section

Calibration measurements were performed after the test section was completed to confirm the comparability of the basic flow in both test sections - in the conventional 2D-adaptive and the new slotted test section. The flows in the empty test sections were compared by using wall pressure measurements and the test section flow was further checked using body pressures of the Cast7 airfoil. All measurements were performed at different Mach numbers using straight, parallel and divergent slots. Fig.- 6 illustrates pressure distributions for the Cast7 airfoil in the 2D and slotted test section for M=0.6 and α=-3° using straight and parallel slots (walls).

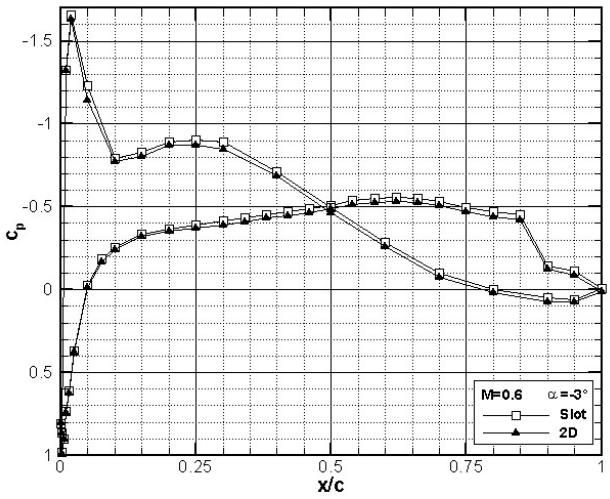

Fig.- 6: Comparison of Cast7 pressure distributions in 2D and slotted test section, α=-3°, M=0.6, straight, parallel walls/slots (calibration)

The step in the data curve near the trailing edge can be attributed to a dent in the airfoil. All investigated calibration configurations properly match, thus it can be assumed that any further deviations during the following tests will be caused by deflected slots.

4. In-slot tests

The in-slot measurements shall yield the actual amount of mass flow that particular slot geometries can accommodate. This will be compared with the mass flow of the appropriate wall deflection in the 2D adaptive test section because any discrepancies will directly affect the actual flow around the test bodies. It is suspected that the main cause for limited adaptation accuracy of adaptive slotted test sections is due to restricted mass flow in the slot.

4.1 Test set-up

Flow velocities in the slot are measured by Laser-2-Focus anemometry (L2F) directly through the access areas in the test section side walls and the vitreous slot walls (see Fig.- 5). The L2F velocity measurements result in a measurement uncertainty of 1m/s for a velocity range up to 330m/s. The basic test set-up is used with the bump on the test section floor and a deviated upper slot [9]. The cross sectional velocity distribution in the slot is measured in three different areas at three different Mach numbers for three different relative slot widths. The slot widths are simply altered with solid slot inserts which have the shape of the slot deflection.

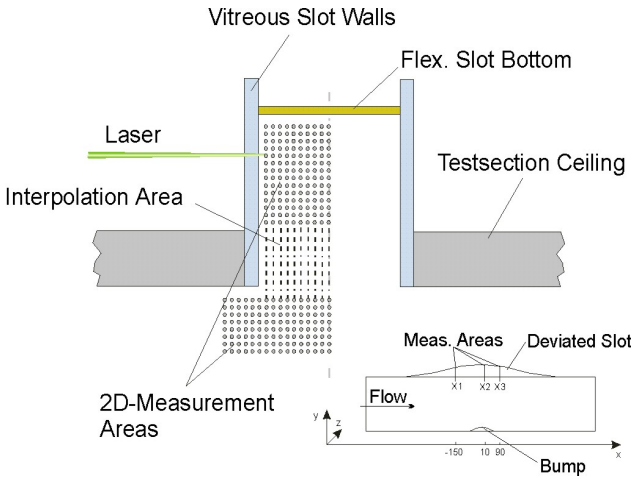

Fig.- 7: Arrangement for in-slot L2F-measurements

Fig.- 7 represents a typical test set-up. The measurement mesh in the slot and the test section is depicted as well as the principle set-up (small image in lower right corner). The velocities are measured as close as possible to the confining slot wall and slot bottom to cover most of the slot area. The symmetry of the slot was utilized for simplicity. The area of the test section ceiling prohibits optical access to parts of the slot. Therefore, the area of the test section ceiling is linearly interpolated using measurements from the extended main test

section area. The distance from the measurement points in the immediate vicinity of the wall/bottom to the actual surfaces, i.e. the rest of the boundary layers, is linearly interpolated as well. The following individual variations were performed:

Table 1: Test cases for in-slot measurements

M	0.4	0.5	0.6
$(b/t)_{min}$	0.19	0.52	0.83
x-pos.	-150	10	90

This results in 27 measurements in the slot, where the x-position describes the relative location with reference to the bump maximum (x=0). The x-positions are chosen to cover areas of the slot inlet, approximate bump-center and outlet.

4.2 Experimental results of in-slot measurements

The velocities in each area were measured for the conditions defined above. An example of a determined velocity field is given in Fig.- 8.

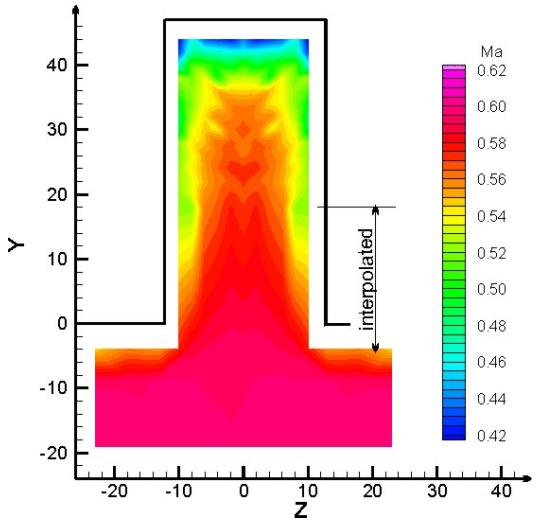

Fig.- 8: Velocity profile in a slot, M_∞=0.6, $(b/t)_{min}$=0.52, x=10mm

The measured areas are simply mirrored at the centerline of the slot and the flow condition in the slot can clearly be observed. The boundary layers at the slot side walls are obvious as is the strongly decelerated flow in the region of the slot bottom. These massive boundary layers are now typical for these slot flows, as the boundary layer observed at the test section ceiling is less developed (thinner). Hence it can be assumed that the actual mass flow in the slot is now less than the theoretical necessary mass flow (area rule) or the mass flow of an adequately deflected 2D wall.

It should also be mentioned that the measured flow patterns coincide in shape with the numerical results in [3]. The question now is, of which magnitude the reduced mass flow in the slot is compared to the adequate flow of the 2D wall deflection.

The mass flow can be calculated from the measured velocities as follows:
The definition of the mass flow is:

$$\dot{m} = \int \rho(u) \cdot u(y,z) dA \qquad (1)$$

where $\rho(u)$ is the local density, $u(y,z)$ the local velocity and dA the distinct areas between the measurement points. An alternative way to write dA is:

$$dA = dz \cdot dy \qquad (2)$$

then the mass flow is:

$$\dot{m} = \int \rho(u) \cdot u(y,z) dz dy \qquad (3)$$

The local densities are calculated from the measured velocities using the isentropic relation:

$$\frac{\rho_0}{\rho} = \left(1 + \frac{\kappa - 1}{2} M^2\right)^{\frac{1}{\kappa - 1}} \qquad (4)$$

The mass flow can now be calculated for half of the slot by numerical integration along the y- and z- direction using the following formula:

$$\frac{\dot{m}_{slot}}{2} = \int \rho(u) \cdot u(y,z) dz dy = \sum_{i,j=1}^{n,m} \left[\frac{\left(\frac{(u \cdot \rho)_i + (u \cdot \rho)_{i+1}}{2} \cdot d \right)_j + \left(\frac{(u \cdot \rho)_i + (u \cdot \rho)_{i+1}}{2} \cdot d \right)_{j+1}}{2} \cdot d \right] \qquad (5)$$

In this formula n and m are the number of measurement points in the z- and y-direction, respectively. These values were set to zero at the slot surfaces to cover half of the slot area.

The appropriate mass flow of a deflected 2D wall was developed in the following manner. The flow velocities outside but still in the vicinity of the slot are very similar to the velocities occurring at the deflected 2D wall (see Fig.- 2 and flow fields in [3]). Therefore, the measured velocities outside the slot were averaged and attributed to a corresponding 2D-test section. Next, the corresponding deflected 2D area was calculated using the area rule and corrected for the boundary layers which occur at the test section side walls. The boundary layer at the ceiling was not considered because this simply shifts upwards. Fig.- 9 depicts this procedure.

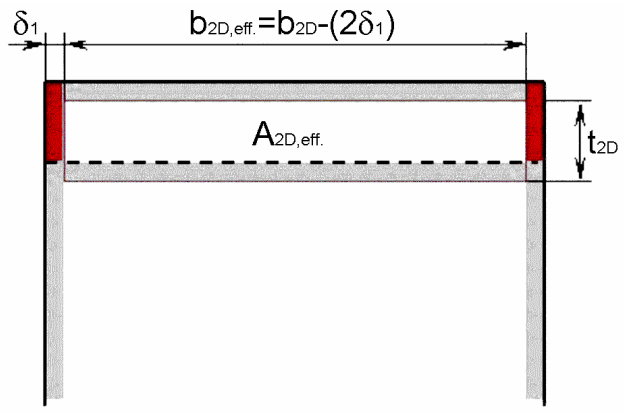

Fig.- 9: Determination of a corresponding area of a 2D wall deflection

Hence, the effective area ($A_{2d,eff.}$) is the area developed from the area rule minus the two amounts calculated from the displacement thickness of the boundary layers at the side walls:

$$A_{2D,eff.} = A_{2D} - \left(2 \cdot \delta_1(x) \cdot t_{2D}\right) \qquad (6)$$

where t_{2D} is the wall displacement and δ_1 is the displacement thickness calculated using Truckenbrodt's relation for turbulent boundary layers [11]:

$$\delta_1 = 0.046 \cdot x \cdot \sqrt[5]{\frac{\nu}{x \cdot u_\infty}} \qquad (7)$$

The average mass flow for a 2D wall deflection is finally calculated from the mean density, the mean velocity and the effective area:

$$\dot{m}_{2D} = \bar{\rho} \cdot \bar{u} \cdot A_{2D,eff.} \qquad (8)$$

The results of the calculated mass flows in the slot are listed in the following table for all parameter variations.

Table 2: Results from slot flow analysis

M	$(b/t)_{min}$	Position x	mass flow in slot [kg/s]	deviation of slot- from 2D mass flow [%]
0.6	0.83	-150	0.217	-10.8
		10	0.315	-10.4
		90	0.279	-10.8
	0.52	-150	0.133	-17.2
		10	0.191	-17.0
		90	0.169	-17.5
	0.19	-150	0.040	-33.4
		10	-	-
		90	-	-
0.5	0.83	-150	0.198	-12.6
		10	0.276	-12.8
		90	0.246	-13.6
	0.52	-150	0.129	-14.5
		10	0.175	-19.8
		90	0.151	-18.5
	0.19	-150	0.036	-35.3
		10	0.047	-41.8
		90	0.048	-33.5
0.4	0.83	-150	0.147	-13.9
		10	0.208	-13.4
		90	0.182	-14.8
	0.52	-150	0.092	-18.9
		10	0.131	-19.6
		90	0.107	-23.1
	0.19	-150	0.027	-35.0
		10	0.033	-44.8
		90	0.036	-33.3

It can be observed that for every combination of Mach number and relative slot width, the deviations in the three measured areas are in the same order. Therefore, for simplicity, the deviations of the three areas are averaged to one value, see Fig.- 10. For the narrow slot at M=0.6, only one area could be measured because it is very difficult to get reasonable signals in the narrow slot due to the strong influence of the boundary layers.

In the former numerical work, predicted trend in mass flow deviation can be seen clearly after comparing the measured slot flow and the estimated 2D-flow (right column). The slenderer the slot, the less the mass can be accommodated when compared to a deflected 2D wall. The same trend applies to decreasing Mach numbers (see Fig.- 10).

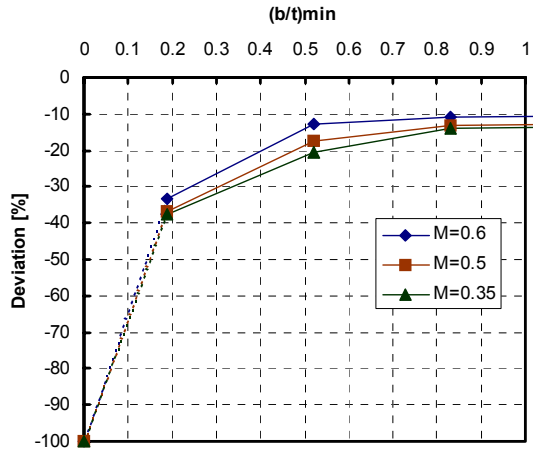

Fig.- 10: Mass flow deficiency in slot compared to 2D wall deflection

The trends are extrapolated to $(b/t)_{min}$= 0 (no slot), which results in a zero mass flow and hence 100% deviation. They can also be extrapolated to the actual 2D-relation of $(b/t)_{min}$ = 11.7 which gives 0% deviation, but the curves will be quite close together with a very flat slope from $(b/t)_{min}$>1 onward. Hence, the most interesting region is the area shown ($0<(b/t)_{min}<1$).

It can be assumed (simplified) that the deficiency in mass flow in the slot must now be covered by the main test section flow in the corresponding area – 'conservation of mass'. Therefore, the amount of mass flow unaccommodated by the slot is added to the flow in the main test section. Regarding the test section size, slot size, number of slots, and mass flow, it should become possible to estimate roughly the average change in velocity over the tested body in the main test section in the area of the slot. The measured pressures and velocities can finally be corrected, regarding all mentioned parameters and the results depicted in Fig.- 10. The following tests should show how accurate slot adaptations appear and whether the correction mentioned above can be applied. The test set-ups were chosen according to the investigated cases in [3].

4.3 Set-up for Cast7 airfoil

The airfoil is first mounted in the 2D-adaptive test section to get the wall and airfoil pressures for the non-adapted, straight and parallel walls for all three Mach numbers (M_∞=0.35, 0.5, 0.6) and one angle of attack (α=-3°). The pressures and the flow fields around the airfoil are measured via a PSI-multichannel pressure acquisition system and the Laser-2-Focus anemometer, respectively.

The interference free wall deflections are calculated using the appropriate adaptation procedure (Amecke, [1]) and applied to the walls. Afterwards, the 2D-wall deflections are transferred via the area rule to the slotted test section and the same measurements are performed again. The advantage of the α=–3° test case is the lack of wall deflections into the test sections.

Fig.- 11 depicts the principle test set-up and the measured L2F area around the Cast7 airfoil. The appropriate slot deflection is indicated as well.

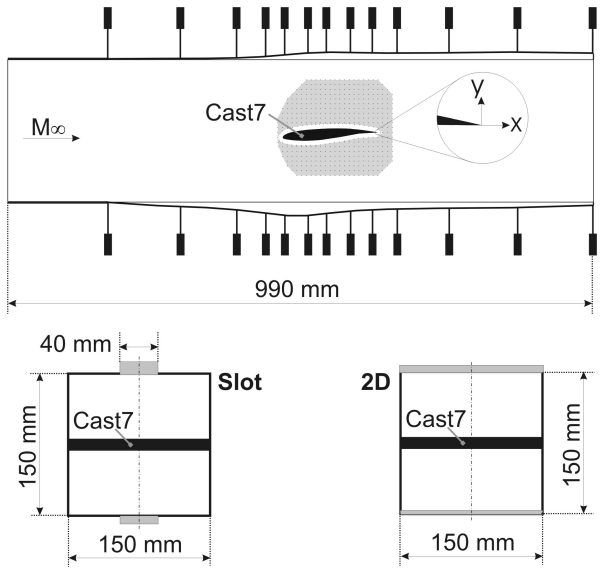

Fig.- 11: Test set-up for Cast7 airfoil measurements, α=-3°

The cross-sectional views in the lower half of Fig.- 11 show the 2D-airfoil in the slotted and the 2D adaptive test section.

4.4 Experimental results of Cast7 airfoil measurements at -3°

The airfoil pressures and flow fields were determined for all Mach numbers at α=–3° in both test sections. An example of the measured flow fields is given in Fig.- 12 and Fig.- 13 in both adapted test sections for M_∞=0.6.

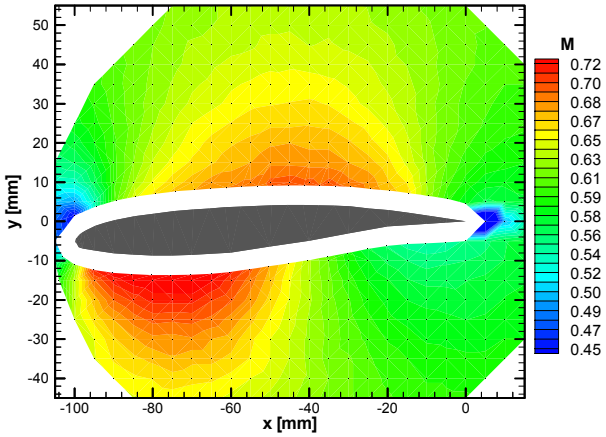

Fig.- 12: Cast7 flow field, 2D test section, M_∞=0.6, α=-3°

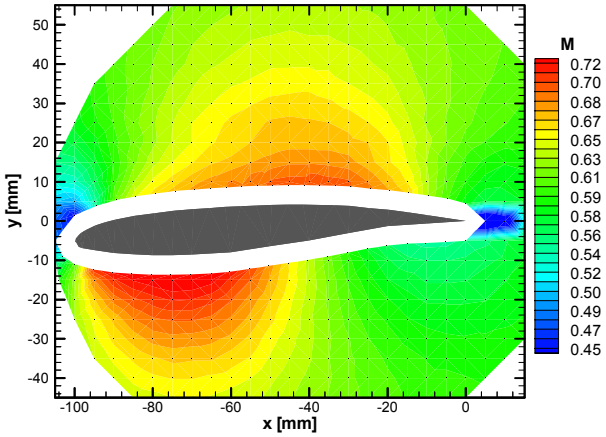

Fig.- 13: Cast7 flow field, slotted test section, M_∞=0.6, α=-3°

The differences in the flow fields (slotted minus 2D) of each test case were calculated to compare and better evaluate the quality of a slot adaptation. Fig.- 14 gives an example of the differences in a flow field in percentage of the local Mach number for one test case.

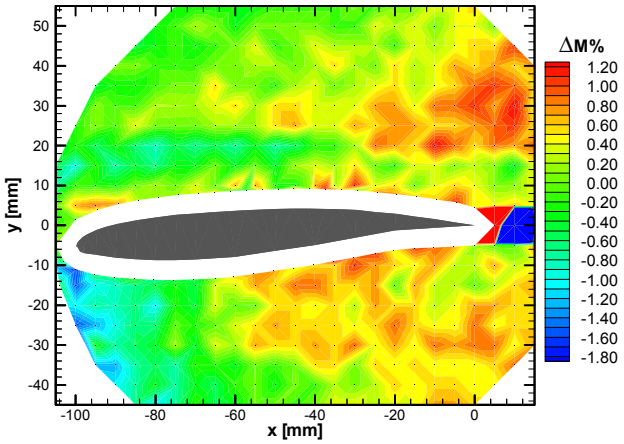

Fig.- 14: Cast7 flow field difference in slotted vs 2D test section, M_∞=0.6, α=-3°

The flow fields show the largest deviations in the wake of the airfoil. These significant deviations can be attributed to the nature of the wake flow and the poor capability of the L2F technique to resolve such flows. This area is therefore ignored in the following analysis. The remaining area indicates the largest deviations in the region of the most prominent velocity gradients, i.e. at the airfoil leading edge. The local differences vary overall between –1.6% to 1.2% maximum. All distinctive deviations in a flow field are averaged now to one value for greater simplicity. This gives the following results for each Mach number:

Table 3: Averaged deviations in flow fields, slot vs 2D adaptation

M_∞	Deviation (slot – 2D) [%]
0.35	1
0.5	0.55
0.6	0.45

The results show a decreasing deviation with increasing Mach number in a range from 1% to 0.45%.

Additionally, the measured pressure distributions show the quality of the investigated adaptations. Fig.- 15 shows the pressure distributions for M_∞=0.6 in the measured unadapted cases (2D & slot), the measured adapted cases, and the numerical result of the single slot adaptation (from [3]).

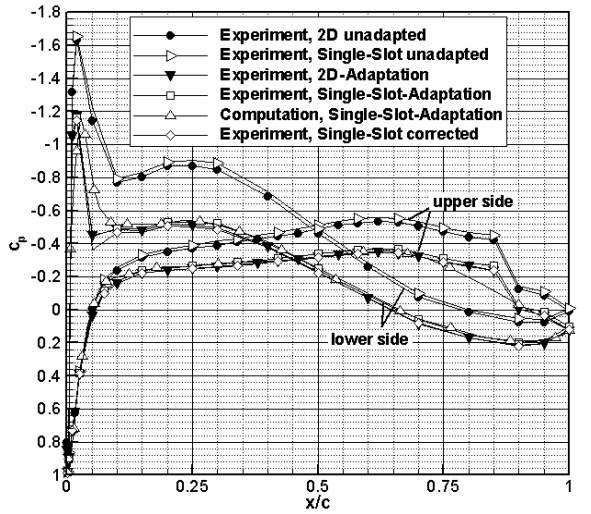

Fig.- 15: Cast7 pressure distributions, 2D vs slotted test section, experiment vs calculation, M_∞=0.6, α=-3°

The slight deviation of the two unadapted curves can be found in the adapted cases as well. Hence, this can not be attributed to the slot adaptation, and the difference must be subtracted from the slot adapted case. Having done this, it is possible to reduce the deviation to that which is induced by the slot adaptation. In summary, a deviation of 1% to 2% in the airfoil pressures can be attributed to the slot adaptation (for all Mach numbers!). This observation agrees with the analyzed results of the flow fields (Table 3).

The small slot deflections with a minimum relative slot width of $(b/t)_{min}$=3.8 do not result in any remarkable change in model flow due to any mass flow deficiencies in the slot as described in the previous chapter. Therefore it is not reasonable to apply any further corrections to this results as the obtained deviations are still in the range of the measurement accuracy.

4.4 First experimental results of Cast7 measurements at 1°

The experimental investigations are extended to an angle of attack of 1° to force stronger wall and slot deflections and additional slot deflections into the test section. The resulting slot deflection into the test section is utilized with a rigid slot inlay mounted to the slot surface as depicted in Fig.- 16.

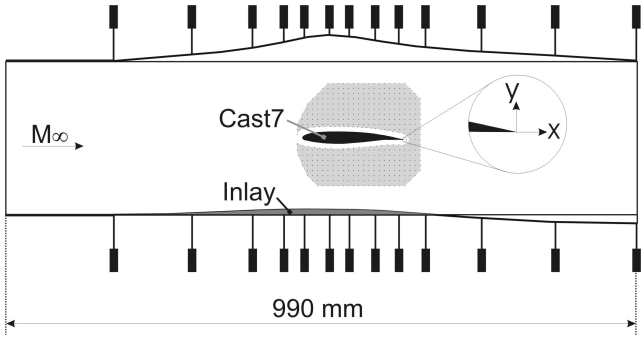

Fig.- 16: Test set-up for Cast7 airfoil measurements with slot inlay, α=1°

The pressure distributions obtained in both test sections are shown in Fig.- 17 for a Mach number of M_∞=0.35. The differences are obtained again in the unadapted case and subtracted from the adapted case to get slot-induced deviations only. Both adapted curves show nearly perfect alignment and the maximum deviations are in the range of <2%.

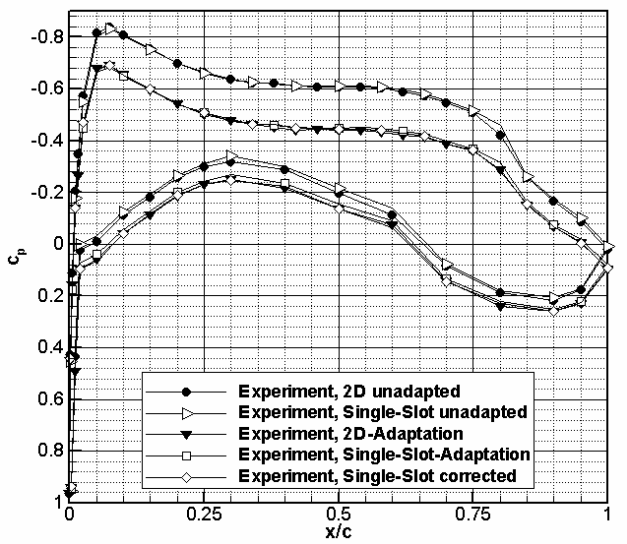

Fig.- 17: Cast7, measured pressure distributions, 2D vs slotted test section, M_∞=0.35, α=1°

5 Conclusions and future work

In the paper it is shown that slot adaptations are successfully feasible within an inaccuracy of 2% compared to the classical 2D wall adaptation. The investigations in the slot indicate the expected growing deviations with the use of slenderer slots (as Futterer predicted in [3]) and show simultaneously a promising way to correct obtained results in adaptive slotted test sections with respect to the applied

parameters, which are the dependency of mass flow deficiency in the slot, slot width and Mach number.

Further work will focus on more detailed measurements with the Cast7 airfoil at a 1° angle of attack. Additionally 3D adaptations will be investigated using the ETB (European Transonic Wind Tunnel Transition Body). The ETB will be designed to match the blockage ratio used in the numerical work in [3]. Furthermore, the advantage of adaptive slots over passive slots will be investigated in the 'Pilot Wind Tunnel' of the ETW (European Transonic Wind Tunnel) using a passive slotted test section. This will finally give a comprehensive picture of the adaptation capabilities of adaptive slots.

Acknowledgements

This work was supported by the German Research Foundation (DFG) in the Special Research Program 557 (SFB557).

References

[1] Amecke J. *Direkte Berechnung von Wandinterferenzen und Wandadaption bei zweidimensionaler Strömung in Windkanälen mit geschlossenen Wänden*, DFVLR-FB 85-62, 1985

[2] Ewald BRF. *Wind Tunnel Wall Corrections*, AGARD-AG-336, (1998)

[3] Futterer I. *Numerische Untersuchung zum Einsatz adaptiver Schlitze zur Minimierung von Windkanalwandinterferenzen bei kompressiblen Unterschallströmungen*, Dissertation TU Berlin, 2000

[4] Ganzer U, Igeta Y, Ziemann J. Design and Operation of TU Berlin Wind Tunnel with Adaptable Walls, *ICAS Paper 84-2.1.1*, 1984

[5] Heddergott A, Kuczka D, Wedemeyer E. The adaptive Rubber Test Section of the DFVLR Göttingen, *IEEE 85CH2210-3* S. 154-156, 1985

[6] Holst H. *Verfahren zur Bestimmung von dreidimensionalen Windkanalwandinterferenzen und Wandadaptionen mit Hilfe gemessener Wanddrücke bei kompressibler Unterschallströmung*, DLR-FB-90-46, 1990

[7] Nitsche W, Wallbruch I, Quest J. Einsatzmöglichkeiten adaptiver Schlitze zur Verringerung von Wandinterferenzen, *DGLR-JT97* 123, München 1997

[8] Meyer O, Futterer I, Nitsche W. Numerische und experimentelle Untersuchungen zum Einsatz adaptiver Schlitze in Windkanalmeßstrecken, *DGLR-JT2000-91*, Dresden 2000

[9] Meyer O, Nitsche W, Futterer I. Numerical and Experimental Investigations on the Reduction of Wind Tunnel Wall Interference by Means of Adaptive Slots, *Aeronautical Journal*, Vol. 105, Nr 1052, , pp571-580, London 2001

[10] Quest J, Nitsche W, Mignosi A. Adaptive Slots: An Alternative Concept to Reduce Wall Interferences, *AGARD-CP-585*, 1996

[11] Truckenbrodt E. *Strömungsmechanik*, Springer-Verlag, 1968

[12] Wolf SWD. *Adaptive Wall Technology for improved Wind Tunnel Testing Techniques - a Review*, Prog. Aerospace Sci. Vol.31 S.85-136, 1995